Inhalation Toxicology, 16:437–445, 2004

ISSN: 0895-8378 print / 1091-7691 online
DOI: 10.1080/08958370490439597

Taylor & Francis
healthsciences

Translocation of Inhaled Ultrafine Particles to the Brain

G. Oberdörster
University of Rochester, Rochester, New York, USA

Z. Sharp, V. Atudorei
University of New Mexico, Albuquerque, New Mexico, USA

A. Elder, R. Gelein
University of Rochester, Rochester, New York, USA

W. Kreyling
National Research Center for Environment and Health (GSF), Neuherberg/Munich, Germany

C. Cox
National Institutes of Health, Bethesda, Maryland, USA

Ultrafine particles (UFP, particles <100 nm) are ubiquitous in ambient urban and indoor air from multiple sources and may contribute to adverse respiratory and cardiovascular effects of particulate matter (PM). Depending on their particle size, inhaled UFP are efficiently deposited in nasal, tracheobronchial, and alveolar regions due to diffusion. Our previous rat studies have shown that UFP can translocate to interstitial sites in the respiratory tract as well as to extrapulmonary organs such as liver within 4 to 24 h postexposure. There were also indications that the olfactory bulb of the brain was targeted. Our objective in this follow-up study, therefore, was to determine whether translocation of inhaled ultrafine solid particles to regions of the brain takes place, hypothesizing that UFP depositing on the olfactory mucosa of the nasal region will translocate along the olfactory nerve into the olfactory bulb. This should result in significant increases in that region on the days following the exposure as opposed to other areas of the central nervous system (CNS). We generated ultrafine elemental ^{13}C particles (CMD = 36 nm; GSD = 1.66) from [^{13}C] graphite rods by electric spark discharge in an argon atmosphere at a concentration of 160 $\mu g/m^3$. Rats were exposed for 6 h, and lungs, cerebrum, cerebellum and olfactory bulbs were removed 1, 3, 5, and 7 days after exposure. ^{13}C concentrations were determined by isotope ratio mass spectroscopy and compared to background ^{13}C levels of sham-exposed controls (day 0). The background corrected pulmonary ^{13}C added as ultrafine ^{13}C particles on day 1 postexposure was 1.34 μg/lung. Lung ^{13}C concentration decreased from 1.39 $\mu g/g$ (day 1) to 0.59 $\mu g/g$ by 7 days postexposure. There was a significant and persistent increase in added ^{13}C in the olfactory bulb of 0.35 $\mu g/g$ on day 1, which increased to 0.43 $\mu g/g$ by day 7. Day 1 ^{13}C concentrations of cerebrum and cerebellum were also significantly increased but the increase was inconsistent, significant only on one additional day of the postexposure period, possibly reflecting translocation across the blood–brain barrier in certain brain regions. The increases in olfactory bulbs are consistent with earlier studies in nonhuman primates and rodents that demonstrated that intranasally instilled solid UFP translocate along axons of the olfactory nerve into the CNS. We conclude from our study that the CNS can be targeted by airborne solid ultrafine particles and that the most likely mechanism is from deposits on the olfactory mucosa of the nasopharyngeal region of the respiratory tract and subsequent translocation via the olfactory nerve.

Received 21 July 2003; sent for revision 13 August 2003; accepted 22 September 2003.

This work was supported by the U.S. Environmental Protection Agency STAR Program, grant R827354, and by NIEHS grant ESO1247. We acknowledge the excellent technical assistance of N. Corson, P. Mercer, and A. Lunts, and the valuable editorial assistance of J. Havalack. The views expressed by the authors are their own and do not necessarily reflect those of the U.S. EPA.

Address correspondence to Dr. Günter Oberdörster, Department of Environmental Medicine, University of Rochester, 575 Elmwood Avenue, Med. Ctr. Box 850, Rochester, NY 14642, USA. E-mail: gunter_oberdorster@urmc.rochester.edu

Depending on particle size, >50% of inhaled UFP can be depositing in the nasopharyngeal region during nasal breathing. Preliminary estimates from the present results show that ~20% of the UFP deposited on the olfactory mucosa of the rat can be translocated to the olfactory bulb. Such neuronal translocation constitutes an additional not generally recognized clearance pathway for inhaled solid UFP, whose significance for humans, however, still needs to be established. It could provide a portal of entry into the CNS for solid UFP, circumventing the tight blood–brain barrier. Whether this translocation of inhaled UFP can cause CNS effects needs to be determined in future studies.

Ultrafine particles (UFP, particles <100 nm) are ubiquitous in the ambient air, both indoor and outdoor, originating from many anthropogenic and natural sources. Several epidemiological studies have shown that ambient UFP are associated with increased respiratory and cardiovascular morbidity and mortality in susceptible people (Wichmann et al., 2000; Peters et al., 1997a, 1997b; Penttinen et al., 2001; von Klot et al., 2002; Pekkanen et al., 2002). The deposition of inhaled UFP in the respiratory tract is governed by diffusional processes, yet there are significant differences within the ultrafine particle size range with respect to the efficiency of their maximal deposition in different regions of the respiratory tract, as depicted in Figure 1. About 90% of inhaled UFP around 1 nm in size deposit in the nasopharyngeal region (Swift et al., 1992; Cheng et al., 1996), whereas only about 10% of this size deposit in the tracheobronchial and essentially none in the alveolar region; in contrast, 5- to 10-nm UFP deposit in all 3 regions with about 20–30% efficiency, whereas 20-nm UFP are predicted to be deposited in the alveolar region up to 50% and only about 10% each in the nasopharyngeal and tracheobronchial regions

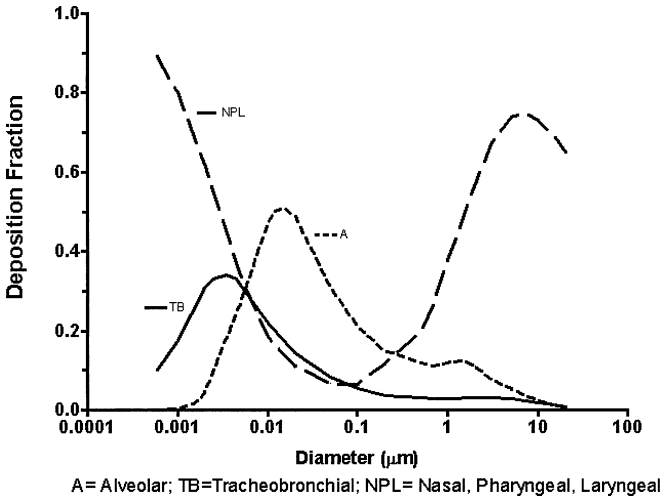

FIG. 1. ICRP (1994) model of fractional depositions of inhaled particles ranging from 0.6 nm to 20 μm in the nasopharyngeal/laryngeal (NPL), the tracheobronchial (TB), and the alveolar (A) regions of the human respiratory tract during nasal breathing. Note that within the ultrafine particle size range (<100 nm) there are significant differences in each of the 3 regions with regard to their deposition probabilities.

(ICRP, 1994). Thus, each of the three regions of the respiratory tract is targeted differently by a given size of UFP (Figure 1). Their fate after deposition seems to differ from that of larger particles, at least as far as solid or poorly soluble UFP are concerned. We have found that within 4 h after whole-body inhalation exposure of rats, ultrafine polytetrafluoroethylene (PTFE) particles (CMD ~ 20 nm) had translocated to submucosal sites of the conducting airways and to the pulmonary interstitium of the alveolar region (Oberdörster et al., 2000). Other rat inhalation studies have shown that ultrafine elemental ^{13}C particles (CMD ~30 nm) had accumulated to a large degree in the liver of rats by 24 h after exposure, indicating efficient translocation into the blood circulation (Oberdörster et al., 2002). Suggested pathways into the blood could be across the alveolar epithelium as well as across intestinal epithelium from particles swallowed into the gastrointestinal (GI) tract. On the other hand, using a method of intratracheal inhalation of ultrafine ^{192}Ir particles in rats, Kreyling et al. (2002) found only minimal translocation (<1%) from the lung to extrapulmonary organs, although they reported 10-fold higher translocation of smaller (15 nm) compared to larger (80 nm) UFP. Nemmar et al. (2002) reported findings in humans that inhalation of ^{99m}Tc-labeled ultrafine carbon particles (Technegas) resulted in the rapid appearance of the label in the blood circulation shortly after exposure and also in the liver. They suggested that this at least partly indicated translocation of inhaled UFP into the blood circulation. In contrast, other studies in humans with ^{99m}Tc-labeled carbon particles (33 nm) by Brown et al. (2002) did not confirm such uptake into the liver, and the authors cautioned that the findings by Nemmar et al. (2002) were likely due to soluble pertechnetate rather than labeled UFP.

It appears, therefore, that UFP size and chemistry (e.g., carbon vs. metal) are important determinants for extrapulmonary translocation of UFP. We had observed in an earlier pilot study with inhaled ultrafine ^{13}C particles a significant increase of ^{13}C in the olfactory bulb of rats, which led us to hypothesize that routes for extrapulmonary translocation of solid UPF other than via the blood circulation exist, that is, involving neuronal pathways from deposits on the nasal olfactory mucosa via the olfactory nerve. We decided, therefore, to conduct a more detailed study in rats with a follow-up period of 7 days after UFP inhalation for measuring their retention in lung and different brain sections. We report here the significant accumulation of ^{13}C in the olfactory bulb over the 7-day postexposure period, suggesting that a most likely pathway of translocation of solid

UFP from the upper respiratory tract is indeed via the olfactory nerve.

METHODS

Generation of Particles

Ultrafine ^{13}C particles were generated from pure [^{13}C] graphite electrodes placed in an electric spark discharge generator supplied with argon in the discharge chamber (Palas soot generator, Karlsruhe, Germany). The [^{13}C]graphite electrodes were made by extruding a slurry of amorphous ^{13}C powder (Isotec, Inc., Miamisburg, OH) mixed with [$^{13}C_6$]glucose (Isotec, Inc., Miamisburg, OH) through a syringe to produce 3.5-mm-diameter cylinders. These were baked in an argon atmosphere by slowly ramping up the temperature to 200°C within 1.5 h in order to degas the extrusion and decompose the glucose. The electrodes were subsequently graphitized at 2400°C in argon.

^{13}C Measurement

Isotopic measurements were performed by continuous-flow isotope ratio mass spectrometry (Brand, 1996), using a Carlo Erba elemental analyzer coupled to a Finnigan Mat Delta Plus mass spectrometer. The results are reported using the conventional δ notation, relative to the PDB standard (fossilized calcite standard), expressed as per mille change:

$$\delta\text{-}^{13}C = \frac{^{13}C/^{12}C_{sample} - ^{13}C/^{12}C_{standard}}{^{13}C/^{12}C_{standard}} \times 1000 \qquad [1]$$

where $^{13}C/^{12}C_{standard}$ is the ratio of the reference material (PDB) and $^{13}C/^{12}C_{sample}$ is the ratio of the sample. Reproducibility was better than 0.1‰ for both standards and samples, which translates into a detection limit of about 1 ppm of added ^{13}C (the $^{13}C/^{12}C$ ratio for PDB is 0.0112372). Since mammalian tissues have a lower $^{13}C/^{12}C$ ratio than the reference carbonate, the δ-^{13}C values are negative.

Animal Exposure and Particle Characterization

Male Fischer-344 rats, 14 wk old, at a body weight of 284 ± 9 g, were used for the study. The exposure was for 6 h in compartmentalized whole-body exposure chambers and was performed in 2 sessions. Particle number concentration in the inhalation chamber was measured by a condensation nuclei counter (TSI model 3022A), and ultrafine particle size distribution by a scanning mobility particle sizer (SMPS, TSI model 3080). Particle mass concentration was determined by an ambient particulate monitor (TEOM, model series 1400a, Rupprecht and Patashnik, Albany, NY). Six rats were exposed in the first session at a concentration of 170 μg ultrafine ^{13}C particles/m^3 (CMD = 37 nm; GSD [geometric standard deviation] = 1.66) and were sacrificed on days 1 and 3 postexposure. An additional 6 rats were exposed in the second session at a concentration of 150 μg ultrafine ^{13}C particles/m^3 (CMD = 35 nm; GSD = 1.66) and were sacrificed on days 5 and 7 postexposure, using 3 rats per time point. Three unexposed rats served as controls.

Organ Preparation and ^{13}C Analysis

At 1, 3, 5, and 7 days postexposure, rats were sacrificed and lung, olfactory bulb, cerebrum, and cerebellum were removed for ^{13}C analysis. The excised organs were weighed. Great care was taken to avoid contamination of the organs with ^{13}C that had deposited on the fur of the animals. To achieve this, the animals were killed by an overdose of intraperitoneal pentobarbital and the fur was wet-wiped with clean tissues. Subsequently the animals were completely skinned and the carcasses were rinsed under water. The carcasses were then moved to a separate clean room and organs were excised there with different clean sets of instruments. The cranium was opened and the cerebrum, cerebellum, and olfactory bulbs were carefully removed. Each of the organs was homogenized with different clean homogenizers and subsequently lyophilized. Unexposed control animals were treated the same way; they were killed prior to sacrificing the day 1 exposed rats. Two 1-mg aliquots of each organ sample were used for δ-^{13}C value determinations using continuous-flow mass spectroscopy for 3–6 replicate measurements. Results were subjected to a weighted two-way analysis of variance (ANOVA), with significant increases in δ-^{13}C values being defined when $p < .05$. The two factors in the ANOVA were exposure group and time. The observations were means of replicate measurements, and the number of replications was used as the weight.

The difference in δ-^{13}C between organs of exposed rats and the average of respective organs of control rats was used to calculate the added ^{13}C organ burden. In order to translate δ-^{13}C values into absolute amounts of ^{13}C added to each organ (excess ^{13}C), the baseline carbon content—that is, the sum of ^{12}C and ^{13}C—of the different organs needs to be known. Such baseline levels are summarized for humans as Reference Man values by ICRP (1992). For example, lung total carbon content is 10% of lung weight, and an average value for brain total carbon content is 12.2% of brain weight. Assuming that the carbon content of organs in rats and humans is the same or very similar, the baseline ^{13}C can be determined using the Reference Man data. These baseline values were used to quantify the added ^{13}C in exposed compared to control animals.

RESULTS

Table 1 shows the results of the δ-^{13}C measurements in lungs and the different sections of the brain of control rats, and of exposed rats on days 1, 3, 5, and 7 postexposure. The lungs display the expected significant increase in δ-^{13}C from −20.28 in controls to −19.04 on day 1. A more than 50% decrease on subsequent days to −19.75 by day 7 follows, still significantly above controls. δ-^{13}C for the olfactory bulb was also significantly elevated on all postexposure days, from a baseline value of −18.91 (controls) to −18.66 (day 1) and to −18.60 (day 7), reflecting the largest increase on day 1

TABLE 1

δ-^{13}C Values and excess ^{13}C levels of lung and brain tissues following 6 h of ultrafine ^{13}C particle exposure (mean ± SD, $n = 3$ per time point)

	Unexposed control; day 0	Postexposure			
		Day 1	Day 3	Day 5	Day 7
Lung					
δ-^{13}C	−20.28 ± 0.27	−19.04 ± 0.23[a]	−19.14 ± 0.24[a]	−19.54 ± 0.14[a]	−19.75 ± 0.14[a]
μg	0.01 ± 0.3	1.34 ± 0.22	1.40 ± 0.31	0.80 ± 0.17	0.64 ± 0.16
μg/g	0.0 ± 0.3	1.39 ± 0.26	1.28 ± 0.27	0.83 ± 0.16	0.59 ± 0.15
Olfactory bulb					
δ-^{13}C	−18.91 ± 0.09	−18.66 ± 0.12[a]	−18.66 ± 0.01[a]	−18.64 ± 0.06[a]	−18.60 ± 0.06[a]
μg	0.00 ± 0.01	0.03 ± 0.02	0.03 ± 0.00	0.03 ± 0.01	0.04 ± 0.01
μg/g	0.01 ± 0.12	0.35 ± 0.17	0.35 ± 0.02	0.37 ± 0.08	0.43 ± 0.08
Cerebrum					
δ-^{13}C	−19.24 ± 0.04	−19.04 ± 0.02[a]	−19.13 ± 0.09	−19.16 ± 0.08	−19.07 ± 0.01[a]
μg	0.00 ± 0.07	0.32 ± 0.02	0.19 ± 0.16	0.14 ± 0.13	0.29 ± 0.02
μg/g	0.00 ± 0.05	0.27 ± 0.03	0.15 ± 0.13	0.11 ± 0.11	0.23 ± 0.02
Cerebellum					
δ-^{13}C	−19.46 ± 0.08	−19.14 ± 0.15[a]	−19.32 ± 0.07	−19.19 ± 0.10[a]	−19.31 ± 0.14
μg	0.00 ± 0.03	0.12 ± 0.04	0.06 ± 0.03	0.10 ± 0.03	0.06 ± 0.06
μg/g	0.00 ± 0.10	0.44 ± 0.20	0.19 ± 0.09	0.37 ± 0.13	0.21 ± 0.19

[a]Significantly increased compared to controls, $p < .05$ (ANOVA).

and continuous slight increases thereafter. Cerebrum and cerebellum also showed increases of δ-^{13}C postexposure, which, however, was not consistent, and significantly elevated only on day 1 (both regions), day 5 (cerebellum), and day 7 (cerebrum). The higher baseline values for δ-^{13}C of the brain regions compared to those in the lungs reflect the greater carbon content of brain tissues compared to that of the lung (ICRP, 1992).

Table 1 and Figure 2 show the results of excess ^{13}C in lung, olfactory bulb, cerebrum, and cerebellum derived from the respective δ-^{13}C values. The day following the 6-h ^{13}C inhalation exposure, an added lung concentration of 1.39 ± 0.26 μg ^{13}C/g lung was determined. By day 7, this concentration had decreased to 0.59 ± 0.15 μg added ^{13}C/g lung. Added ^{13}C concentrations in the olfactory bulb were significantly increased throughout the postexposure period, increasing to 0.35 ± 0.17 μg/g tissue on day 1 and to 0.43 ± 0.08 μg/g tissue by day 7. Added ^{13}C concentrations in cerebellum and cerebrum were significantly elevated only on 2 of the postexposure days, reaching concentrations between 0.11 and 0.44 μg/g tissue.

Although by day 7 the olfactory bulb concentration of ^{13}C approached day 7 ^{13}C concentrations in the lung, the total amount accumulating in the olfactory bulb is only small; considering its average weight of only 85 mg, the amount accumulating in the olfactory bulb over 7 days was 40 ng (Table 1). This, however, was achieved after a single exposure only, and since no decrease in ^{13}C during the 7 days postexposure occurred, continuous exposures are likely to reach much higher levels. Due to the greater weight of cerebrum and cerebellum, their total ^{13}C content on day 1 postexposure was calculated to be 10- and 4-fold higher compared to the olfactory bulb (Table 1). However, this elevation was not consistently significant over the

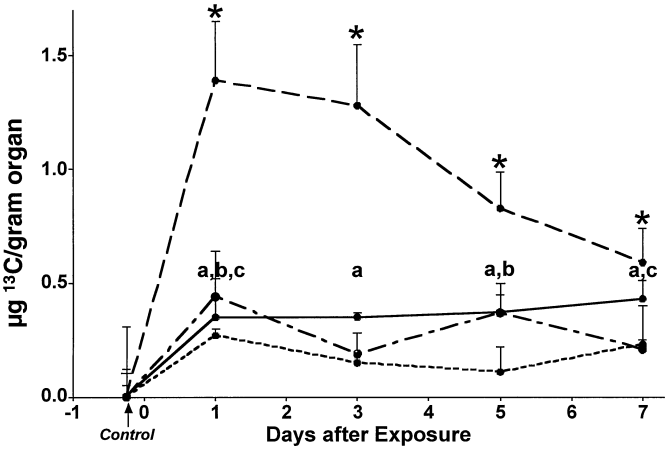

FIG. 2. Time course of ^{13}C tissue concentrations in lung, olfactory bulb, cerebrum, and cerebellum of rats following a 6-h inhalation exposure to ultrafine (36 nm CMD) elemental ^{13}C particles ($n = 3$ rats per time point): – – lung;—olfactory—– — –cerebellum; ⋯ cerebrum. Asterisk and *a*, *b*, *c* indicate values significantly greater than controls, $p < .05$ (ANOVA) (asterisk for lung, *a* for olfactory bulb, *b* for cerebellum, *c* for cerebrum).

following days; it may well reflect some localized higher accumulation, which needs to be further investigated in subsequent studies.

DISCUSSION

We found significant and continuous increases of ^{13}C in the olfactory bulb throughout the 7-day postexposure period following the 6-h inhalation exposure to ultrafine elemental ^{13}C particles with a CMD of 36 nm and GSD of 1.66. Cerebrum and cerebellum also showed significant increases on 2 of the postexposure days. Since elemental carbon is insoluble (CRC Press, 2000), these changes in ^{13}C concentration reflect the accumulation and retention of the ultrafine carbon particles in the respective organs. Translocation of the inhaled ultrafine carbon particles to the CNS could occur principally via two pathway: One is through access across the blood–brain barrier (BBB) of ultrafine particles after their translocation into the blood circulation from deposits anywhere in the respiratory tract; the other—specific for the olfactory bulb—is via the olfactory nerve from deposits on the nasal olfactory mucosa the third pathway is *via* paracellular or perineural pathways across the olfactory mucosa and ethmoid bone into cerebrospinal fluid (CSF) (Illum, 2000). Although our present study was not designed to differentiate between these three pathways, we offer the following interpretation of our results based on available literature data.

Supportive of a circulatory route of UFP translocation from deposits in the respiratory tract are results of our previous study (Oberdörster et al., 2002). Significant amounts of ultrafine ^{13}C accumulated in the liver by 24 h postexposure, which must be a consequence of the ultrafine carbon particles having translocated into the blood circulation. Against the circulatory route of CNS translocation of UFP speaks the fact that the BBB is very tight, and studies with iv-injected UFP failed to demonstrate their access into the CNS across this barrier (Gulyaev et al., 1999) or across the tight distal barrier of the basal lamina (Muldoon et al., 1999). Only after coating intravenously injected nanoparticles with polysorbate or apolipoprotein did they seem to mimic lipoprotein particles that could be taken up by brain capillary endothelial cells via receptor-mediated phagocytosis (Kreuter et al., 2002). Yet even then, transcytosis of the nanoparticles across the BBB could not be demonstrated. Particles translocating along paracellular or perineural pathways into CSF would have to cross the CSF-brain barrier, another functional barrier, and would not target specifically the olfactory bulb. Thus, the consistent postexposure increase of ^{13}C in the olfactory bulb is unlikely to be of blood-borne CSF origin. It is conceivable, though, that the increase in ^{13}C in cerebrum and cerebellum in our study reflects some translocation of solid UFP across the BBB in regions where epithelia are less tight, such as the circumventricular organs, or across the blood-CSF barrier, such as the choroid plexus, ventricles, brainstem centers, and hypothalamus (Segal, 2000; Ueno et al., 2000). Possible translocation from the blood circulation in these areas may be associated with a very rapid clearance from the lung early during the exposure of more than 50% of the UFP depositing in the lung. Such early rapid clearance was suggested by the results of our previous study (Oberdörster et al., 2002) based on the difference between measured and predicted lung burden. The present study, too, shows a large difference between the predicted deposition of ^{13}C in the lung (2.93 μg)* and what was actually measured on day 1 (1.34 μg; Table 1), which suggests, assuming that the model is correct, more than 50% elimination of pulmonary ^{13}C during the exposure phase. If most of this is translocated into the blood circulation, some transport across the less developed sections of the BBB conceivably may occur. This could then account for the increased ^{13}C levels in cerebrum and cerebellum on day 1 postexposure. However, since only the olfactory bulbs showed consistent and increasing ^{13}C levels on all days in the 7-day postexposure period, and cerebellum and cerebrum only on 1 day, we believe that at least for the olfactory bulb, axonal transport of UFP via olfactory neurons from nasal deposits into the CNS is the major translocation mechanism.

The existence of an olfactory nerve pathway as access to the CNS has been well demonstrated for inhaled or nasally instilled soluble metal compounds (Tjälve & Henriksson, 1999; Arvidson, 1994; Dorman et al., 2002). Since inhalation exposure of UFP results in significant deposition in the nasal area of the rat, a reasonable interpretation of our result is that inhaled solid UFP translocate via this route as well. In order to prove that nasal deposits of UFP translocate to the olfactory bulb, it would be most convincing to demonstrate the presence of the ultrafine ^{13}C particles in the axons of the olfactory neurons. While our present study was limited in its design and did not include dissection and analysis of olfactory nerves, the older literature provides convincing evidence for such neuronal translocation of solid UFP following intranasal instillations in nonhuman primates and in rats.

De Lorenzo (1970) in a landmark study demonstrated in squirrel monkeys that intranasally instilled colloidal gold particles (50 nm) translocated anterogradely in the axons of the olfactory nerves to the olfactory bulbs. He used transmission electron microscopy to image the sequence of the passage of the 50-nm electron-dense particles along the whole pathway: starting with their localization postinstillation on the olfactory mucosa, followed by uptake into the olfactory rods of the nasal mucosa (probably via endocytosis as evidenced by large numbers of pinocytotic vacuoles, which led the author to conclude that "the olfactory rod is busily engaged in "drinking in" from the extracellular environment"), retrograde translocation within the olfactory dendrites likely associated with microtubuli, anterograde movement in the axoplasm along the olfactory fila of the olfactory nerve, appearance in the olfactory bulb, and then even showing the 50 nm gold particles having crossed synapses

*This prediction is based on the multiple path particle deposition model (Asgharian et al., 1999) with 0.55 μg ^{13}C-UFP depositing in the tracheobronchial region and 2.38 μg in the alveolar region of the rats during the 6-h exposure.

in the olfactory glomerulus to reach mitral cell dendrites within 1 h after intranasal instillation. An interesting finding in this study—and important for potential adverse effects—was that the UFP in the olfactory bulb were no longer freely distributed in the cytoplasm but were preferentially located in mitochondria. Remarkable also is the neuronal transport velocity of the 50 nm gold particles, calculated by De Lorenzo to be 2.5 mm/h.

Other studies on olfactory translocation of solid UFP were reported in the 1940s and concerned a large series of studies with 30 nm polio virus intranasally instilled into chimpanzees and Rhesus monkeys (Bodian & Howe, 1941; Howe & Bodian, 1941). Their studies revealed that the olfactory nerve and olfactory bulbs are, indeed, portals of entry to the CNS for the intranasally-instilled ultrafine polio virus particles, which could subsequently be recovered from the olfactory bulbs. The transport velocity of the virus in the axoplasm of axons was determined at 2.4 mm/h, which is very well in agreement with De Lorenzo's result, and also with neuronal transport velocities measured later by Adams and Bray (1983) for solid particles (up to 500 nm) directly microinjected into giant axons of crabs.

There are additional studies showing that sensory nerves in the upper and lower respiratory tract can take up solid micro particles and translocate these. For example, a more recent study by Hunter and Dey (1998) in rats demonstrated the translocation of intranasally instilled rhodamine-labeled microspheres (20–200 nm) to the trigeminal ganglion inside the cranium via uptake into the ophthalmic and maxillary neurons of the trigeminus nerve. The trigeminus supplies sensory nerve endings throughout the nasal mucosa, including the olfactory mucosa (Shankland, 2001; Schaefer et al., 2002). Hunter and Undem (1999) in a different study instilled the same microparticles intratracheally into guinea pigs. They found that sensory nerves supplying the tracheobronchial region with a dense network can take up and translocate these solid microparticles to the ganglion nodosum in the neck area, which is networked into the vagal system. Their method of tracing neuronal pathways had been developed by Katz et al. (1984), who had shown that these rhodamine-labeled microparticles (30 nm may be the optimal size; Katz, personal communication) translocated along axons and dendrites when microinjected into cortical sections of rats and cats.

Collectively, these studies show that solid UFP of different materials can effectively be taken up by sensory nerve endings at several sites in the respiratory tract and gain access to the CNS and ganglionic structures. In particular, the studies by De Lorenzo (1970) demonstrate unequivocally the existence of a neuronal olfactory pathway to the CNS for nasally deposited solid UFP. Since inhaled UFP are deposited to a significant degree in the nasal region of the respiratory tract of the rat (Gerde et al., 1991), a most likely mechanism to explain the ^{13}C accumulation in the olfactory bulb of rats in our inhalation study is via the olfactory neuronal route. Possibly, differences in the physicochemical nature of UFP may influence such translocation.

In an attempt to quantify the translocation of ^{13}C particles along this pathway in our study we considered the following: Nasal deposition studies of ultrafine particles in rats showed that the deposition efficiency for 42-nm particles is 10.5% (Gerde et al., 1991). The CMD of the ultrafine ^{13}C particles in our study was 36 nm, with a geometric standard deviation of 1.66. A recently developed particle deposition model (MPPD, multiple path particle deposition; Asgharian et al., 1999) predicts for the rat that at this particle size distribution 9.4% of the inhaled particles will deposit in the nasal compartment, including the nasal olfactory mucosa close to the measured value by Gerde et al. (1991). Under our specific study conditions, this amounts to 1.10 μg of ultrafine ^{13}C particles, which is almost as much as was measured in the lung. Since only 15% of the total airflow is directed to the olfactory mucosa in rats (Kimbell et al., 1997), the predicted deposited amount of ^{13}C in this area may only be 165 ng, 15% of the total nasal deposit. Assuming that the amount of ^{13}C measured in the olfactory bulb (30–40 ng, Table 1) was translocated along the olfactory neuronal route, this would mean that $\sim$20% of the deposited amount on the olfactory mucosa was translocated to the olfactory bulb over the 7-day postexposure period. There are probably significant uncertainties around this estimate and therefore it has to be viewed with caution. Additional studies using more sensitive methods of detection are required to verify translocation pathways and more precisely quantitate neuronal translocation efficiency of inhaled UFP.

Considering that only 5% of the human nasal mucosa is olfactory epithelium as opposed to 50% in rats (Keyhani et al., 1997; Kimbell et al., 1997), one can question the importance of olfactory nerve translocation for UFP in humans. In addition, rats are obligatory nose breathers, whereas humans are mixed oro-nasal/nasal breathers. However, although only 15% of the total rat nasal airflow is directed to their olfactory mucosa, it is 10% in humans (Keyhani et al., 1997; Kimbell et al., 1997), only one-third less. Moreover, as pointed out before, the rest of the nasal mucosa is supplied by sensory nerve endings of the ophthalmic and maxillary branches of the trigeminus nerve, which can also function as a translocation pathway for solid UFP as discussed earlier (Hunter & Dey, 1998). Some of the trigeminal sensory nerve endings in the nasal epithelium also have branches reaching directly into the olfactory bulb (Schaefer et al., 2002).

Classical clearance mechanisms for inhaled particles deposited in the nasal compartment of the respiratory tract are via mucociliary transport (toward the oropharynx in the posterior part of the nose, and through sneezing and nose blowing. Biosoluble components of particles deposited in this region are subjected to dissolution and subsequent absorption into blood (U.S. EPA, 1996; Schlesinger et al., 1997). Uptake by sensory nerve endings (olfactory, trigeminus), which has been the focus of this discussion, constitutes a clearance pathway to extrapulmonary organs, that is, the CNS, which has not been appropriately recognized so far, despite several recent reports describing

the passage of metals along this route after inhalation or nasal instillation of biosoluble metal compounds (Gianutsos et al., 1997; Tjälve & Henriksson, 1999; Brenneman et al., 2000; Dorman et al., 2002). Dorman et al. (2002) pointed out most recently the potential importance of this pathway for brain delivery of Mn derived from soluble and slowly soluble inhaled Mn compounds. That this delivery route exists as well for solid UFP is clearly demonstrated by the earlier work on olfactory uptake and transport of 50-nm gold particles and 30-nm virus particles described above (Bodian & Howe, 1941; Howe & Bodian, 1941; De Lorenzo, 1970); also, our present result with 36-nm insoluble elemental carbon particles is consistent with this same translocation mechanism and extends the earlier findings from nasally instilled to inhaled UFP. Thus, the olfactory route to the CNS and uptake into other sensory nerve endings in the extrathoracic and tracheobronchial region should be recognized as mechanisms for extrapulmonary translocation of soluble metal compounds and UFP (Figure 3), in addition to the "classical" clearance mechanism in the nasal area already mentioned.

Neuronal uptake and translocation in the respiratory tract could be especially important for the smallest UFP below 10–20 nm generated at very high number concentrations in the ambient air from traffic-related sources and photochemical nucleation events (Kittelson, 1998; McMurry et al., 2000; Woo et al., 2001), or for newly developed nanomaterials (engineered nanoparticles of carbon, metals, metal oxides, quantum dots etc.) should they become airborne and be inhaled. The smaller the inhaled UFP, the more of them could be subjected to a neuronal clearance pathway in the nose, because nasal deposition increases with decreasing UFP size. Below a size of 5 nm, nasal deposition efficiency rises rapidly and eventually approaches 100%, whereas particles above 30 nm have only a less than 10% nasal deposition probability (Figure 1); (ICRP, 1994; Cheng et al., 1996; Swift et al., 1992). Since the smaller ambient UFP consist of very little elemental but mostly organic carbon (Kittelson, 1998), their fate after deposition depends most likely on their lipid or water dissolution rate; that is, how long after deposition will these particles maintain their particulate state: are they dissolving quickly before translocation, during translocation, or once they have reached CNS structures? Even if dissolution occurs during the translocation process, anterograde translocation and retrograde translocation of lipids and organic material along axons of neurons have been shown to take place as well (Grafstein & Foreman, 1980).

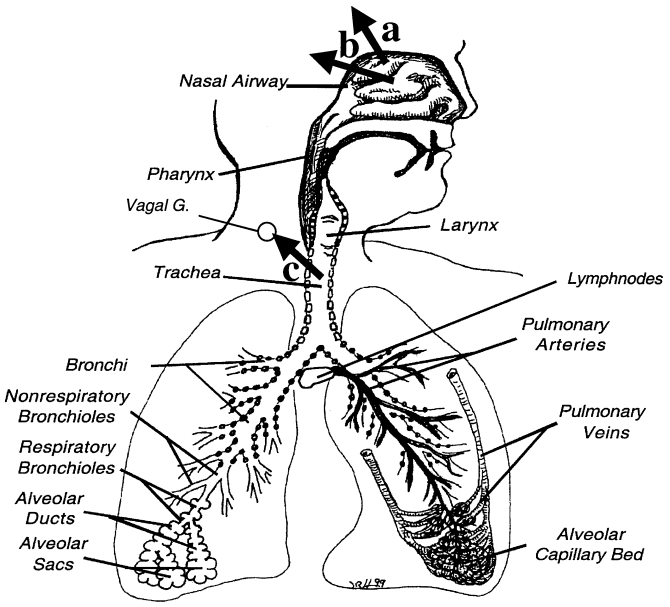

FIG. 3. Suggested neuronal translocation pathways in humans for solid nanosized particles and for soluble components of larger particles that have been demonstrated in rodents and nonhuman primates. These include uptake into nerve endings embedded in mucosa of nasal (*a*, olfactory; *b*, trigeminal nerves) and tracheobronchial (*c*, afferent vagal nerves) region. The biological/toxicological importance of these pathways and their contribution to particle clearance vis-à-vis the classical clearance pathways of mucociliary and phagocytic cell transport, dissolution, diffusion, and protein binding remain to be determined. Drawing courtesy of Dr. J. Harkema.

While the early studies—showing nasal to olfactory bulb translocation of 30-nm virus and 50-nm gold particles in nonhuman primates—prove that this transfer mechanism operates in primates, the significance for humans still needs to be established. In general, there are many unanswered questions regarding sensory nerve uptake and transport of inhaled UFP deposited on the mucosa of the olfactory nasal region and at other sites of the respiratory tract, including: What is the mechanism of uptake: receptor-mediated endocytosis, pinocytosis, axonal transport? How do physicochemical characteristics of UFP and their surfaces influence uptake and translocation? How far into the CNS—beyond he olfactory bulb to striatal, frontal cortex, and other structures—can UFP be translocated? To what extent is this pathway operable for volatile and semivolatile organics as major constituents of ambient UFP below ~20 nm? Are there toxicological consequences? A recent study described significant inflammatory changes of the olfactory mucosa, olfactory bulb, and cortical and subcortical structures in dogs from a heavily polluted area in Mexico City, changes that were not seen in dogs from a less polluted control city (Calderon-Garciduenas et al., 2002). While this study was not designed to investigate a nasal-CNS transfer route of inhaled ultrafine particulate air pollutants, the observed inflammatory changes are consistent with such mechanism. Is UFP uptake limited to particles <100 nm, or does this mechanism also operate for larger particles? Axonal diameter certainly will impose a limit—for example, olfactory fila in the squirrel monkey measure 200 nm in diameter (DeLorenzo, 1970). Anterograde and retrograde transport of even larger particles directly injected into a giant axon has been observed (Adams & Bray, 1983), with one suggested mechanism being cytoskeletal movement along an escalator provided by axonal and dendritic microtubuli (Hirokawa, 1998; Ligon

& Steward, 2000) via kinesin and cytoplasmic dynein motor proteins (Vale et al., 1985; Paschal et al., 1987). Protein coating of UFP after deposition may be necessary for this neuronal translocation pathway. In addition, the vascular route of translocation, that is, UFP crossing the BBB after entering the vascular compartment, needs to be explored as well. Answers to these questions of are interest not only for ambient UFP but also for the growing field of biomedical use of engineered nanoparticles and quantum dots with respect to their kinetics when administered in vivo as drug delivery devices or as biosensors.

We conclude from our studies that inhaled ultrafine carbon particles are to a significant extent translocated to the CNS. Our findings are consistent with retrograde dendritic and anterograde axonal transport via the olfactory nerve, a pathway whose existence in non-human primates and in rodents has been proven in earlier nasal instillation studies for solid UFP as well as for soluble metal compounds. This constitutes a direct portal of entry for UFP into the CNS, circumventing the tight blood–brain barrier. This not generally recognized clearance pathway from the nasal mucosa to the CNS could be of significance for induction of neurotoxic effects following acute or chronic inhalation exposures to environmental or occupational UFP. Potential long-term effects of their accumulation in the olfactory bulb and translocation to other regions of the CNS represent a new field in PM research.

REFERENCES

Adams, R. J., and Bray, D. 1983. Rapid transport of foreign particles microinjected into crab axons. *Nature* 303:718–720.

Arvidson, B. 1994. A review of axonal transport of metal. *Toxicology* 88:1–14.

Asgharian, B., Miller, F. J., Subramaniam, R. P., Dosimetry software to predict particle deposition in humans and rats. CIIT Activities, Vol 19, No. 3, March, 1999.

Bodian, D., and Howe, H. A. 1941. The rate of progression of poliomyelitis virus in nerves. *Bull. Johns Hopkins Hosp.* LXIX(2):79–85.

Brand, W. A. 1996. High precision isotope ratio monitoring techniques in mass spectrometry. *J. Mass Spectrom.* 31:225–235.

Brenneman, K. A., Wong, B. A., Buccellato, M. A., Costa, E. R., Gross, E. A., and Dorman, D. C. 2000. Direct olfactory transport of inhaled manganese ($^{54}MnCl_2$) to the rat brain. Toxicokinetic investigations in a unilateral nasal occlusion model. *Toxicol. Appl. Pharmacol*. 169:238–248.

Brown, J. S., Zeman, K. L., and Bennett, W. D. 2002. Ultrafine particle deposition and clearance in the healthy and obstructed lung. *Am. J. Respir. Crit. Care Med.* 166:1240–1247.

Calderon-Garciduenas, L., Azzarelli, B., Acune, H., Garcia, R., Gambling, T. M., Osnaya, N., Monroy, S., Tizapantzi, M. D. R., Carson, J. L., Villarreal-Calderon, A., and Rewcastle, B. 2002. Air pollution and brain damage. *Toxicol. Pathol.* 30(3):373–389.

Cheng, Y.-S., Yeh, H.-C., Guilmette, R. A., Simpson, S. Q., Cheng, K. H., and Swift, D. L. 1996. Nasal deposition of ultrafine particles in human volunteers and its relationship to airway geometry. *Aerosol Sci. Technol.* 25:274–291.

CRC Press. 2000. *CRC handbook of chemistry & physics*. *A ready-reference book of chemical and physical data*, 81st ed. Boca Raton, FL: CRC Press.

De Lorenzo, A. J. D. 1970. The olfactory neuron and the blood–brain barrier. In *Taste and smell in vertebrates*. eds. G. E. W. Wolstenholme and J. Knight, pp. 151–176. CIBA Foundation Symposium Series. J.&A. Churchill, London.

Dorman, D. C., Brenneman, K. A., McElveen, A. M., Lynch, S. E., Roberts, K. C., and Wong, B. A. 2002. Olfactory transport: A direct route of delivery of inhaled manganese phosphate to the rat brain. *J. Toxicol. Environ. Health A* 65(20):1493–1511.

Gerde, P., Cheng, Y. S., and Medinsky, M. A. 1991. *In vivo* deposition of ultrafine aerosols in the nasal airway of the rat. *Fundam. Appl. Toxicol.* 16:330–336.

Gianutsos, G., Morrow, G. R., and Morris, J. B. 1997. Accumulation of manganese in rat brain following intranasal administration. *Fundam. Appl. Toxicol.* 37:102–105.

Grafstein, B., and Forman, D. S. 1980. Intracellular transport in neurons. *Physiol. Rev.* 60(4):1167–1283.

Gulyaev, A. E., Gelperina, S. E., Skidan, I. N., Antropov, A. R., Kivman, G. Y., and Kreuter, J. 1999. Significant transport of doxorubicin into the brain with polysorbate 80-coated nanoparticles. *Pharm. Res.* 16(10):1564–1569.

Hirokawa, N. 1998. Kinesin and dynein superfamily proteins and the mechanism of organelle transport. *Science* 279:519–526.

Howe, H. A., and Bodian, D. 1941. Poliomyelitis in the chimpanzee: A clinical–pathological study. *Bull. Johns Hopkins Hosp.* LXIX(2):149–182.

Hunter, D. D., and Dey, R. D. 1998. Identification and neuropeptide content of trigeminal neurons innervating the rat nasal epithelium. *Neuroscience* 83(2):591–599.

Hunter, D. D., and Undem, B. J. 1999. Identification of substance P content of vagal afferent neurons innervating the epithelium of the guinea pig trachea. *Am. J. Respir. Crit. Care Med*. 159:1943–1948.

ICRP. 1992. *International Commission on Radiological Protection, No. 23, Report of the Task Group on Reference Man*. New York: Pergamon Press.

ICRP. 1994. Human respiratory tract model for radiological protection. *Ann. ICRP* 24(1–3). ICRP publication 66.

Illum, L. 2000. Transport of drugs from the nasal cavity to the central nervous system. *European Journal of Pharmaceutical Sciences* 11:1–18.

Katz, L. C., Burkhalter, A., and Dreyer, W. J. 1984. Fluorescent latex microspheres as a retrograde neuronal marker for *in vivo* and *in vitro* studies of visual cortex. *Nature* 310:498–500.

Keyhani, K., Scherer, P. W., and Mozell, M. M. 1997. A numerical model of nasal odorant transport for the analysis of human olfaction. *J. Theor. Biol*. 186:279–301.

Kimbell, J. S., Godo, M. N., Gross, E. A., Joyner, D. R., Richardson, R. B., and Morgan, K. T. 1997. Computer simulation of inspiratory airflow in all regions of the F344 rat nasal passages. *Toxicol. Appl. Pharmacol.* 145:388–398.

Kittelson, D. V. 1998. Engines and nanoparticles: A review. *J. Aerosol Sci.* 29(5,6):575–588.

Kreuter, J., Shamenkov, D., Petrov, V., Ramge, P., Cychutek, K., Koch-Brandt, C., and Alyautdin, R. 2002. Apolipoprotein-mediated

transport of nanoparticles-bound drugs across the blood–brain barrier. *J. Drug Targeting* 10(4):317–325.

Kreyling, W. G., Semmler, M., Erbe, F., Mayer, P., Takenaka, S., Schulz, H., Oberdörster, G., and Ziesenis, A. 2002. Ultrafine insoluble iridium particles are negligibly translocated from lung epithelium to extrapulmonary organs. *J. Toxicol. Environ. Health A* 65(20):1513–1530.

Ligon, L. A., and Steward, O. 2000. Movement of mitochondria in the axons and dendrites of cultured hippocampal neurons. *J. Comp. Neurol.* 427:340–350.

McMurry, P. H., Woo, K. S., Weber, R., Chen, D.-R., and Pui, D. Y. H. 2000. Size distributions of 3 to 10 nm atmospheric particles: Implications for nucleation mechanisms. *Philos. Trans. R. Soc. Lond. Ser. A* 358:2625–2642.

Muldoon, L. L., Pagel, M. A., Kroll, R. A., Roman-Goldstein, S., Jones, R. S., and Neuwelt, E. A. 1999. A physiological barrier distal to the anatomic blood–brain barrier in a model of transvascular delivery. *Am. J. Neuroradiol.* 20:217–222.

Nemmar, A., Hoet, P. H. M., Vanquickenborne, B., Dinsdale, D., Thomeer, M., Hoylaerts, M. F., Vanbilloen, H., Mortelmans, L., Nemery, B. 2002. Passage of inhaled particles into the blood circulation in humans. *Circulation* 105:411–414.

Oberdörster, G., Finkelstein, J. N., Johnston, C., Gelein, R., Cox, C., Baggs, R., and Elder, A. C. P. 2000. *HEI research report: Acute pulmonary effects of ultrafine particles in rats and mice*. Research Report 96, August. Health Effects Institute, www.healtheffects.org/pubs-research.htm

Oberdörster, G., Sharp, Z., Atudorei, V., Elder A., Gelein, R., Lunts, A., Kreyling, W., and Cox, C. 2002. Extrapulmonary translocation of ultrafine carbon particles following whole-body inhalation exposure of rats. *J. Toxicol. Environ. Health A* 65(20):1531–1543.

Paschal, B. M., Shpetner, H. S., and Vallee, R. B. 1987. MAP 1C is a microtubule-activated ATP-ase which translocates microtubules *in vitro* and has dynein-like properties. *J. Cell Biol*. 105:1273–1282.

Pekkanen, J., Peters, A., Hoek, G., Tiittanen, P., Brunekreef, B., de Hartog, J., Heinrich, J., Ibald-Mulli, A., Kreyling, W. G., Lanki, T., Timonen, K. L., and Vanninen, E. 2002. Particulate air pollution and risk of ST-segment depression during repeated submaximal exercise tests among subjects with coronary heart disease. The exposure and risk assessment for fine and ultrafine particles in ambient air (ULTRA) study. *Circulation* 106:933–938.

Penttinen, P., Timonen, K. L., Tiittanen, P., Mirme, A., Ruuskanen, J., and Pekkanen, J. 2001. Ultrafine particles in urban air and respiratory health among adult asthmatics. *Euro. Respir. J.* 17(3):428–435.

Peters, A., Wichmann, H. E., Tuch, T., Heinrich, J., and Heyder, J. 1997a. Respiratory effects are associated with the number of ultrafine particles. *Am. J. Respir. Crit. Care Med*. 155:1376–1383.

Peters, A., Doring, A., Wichmann, H.-E., and Koenig, W. 1997b. Increased plasma viscosity during an air pollution episode: A link to mortality? *Lancet* 349(9065):1582–1587.

Schaefer, M. L., Bottger, B., Silver, W. L., and Finger, T. E. 2002. Trigeminal collaterals in the nasal epithelium and olfactory bulb: A potential route for direct modulation of olfactory information by trigeminal stimuli. *J. Comp. Neurol*. 444(3):221–226.

Schlesinger, R. B., Ben-Jebria, A., Dahl, A. R., Snipes, M. B., and Ultman, J. 1997. Disposition of inhaled toxicants. In *Handbook of human toxicology*, ed E. J. Massaro, pp. 493–550. Boca Raton, FL: CRC Press.

Segal, M. B. 2000. The choroid plexuses and the barriers between the blood and the cerebrospinal fluid. *Cell. Mol. Neurobiol*. 20(2):183–196.

Shankland, W. E. 2001. The trigeminal nerve. Part III: The maxillary division. *Cranio* 19(2):78–83.

Swift, D. L., Montassier, N., Hopke, P. K., Karpen-Hayes, K., Cheng, Y.-S., Su, Y. F., Yeh, H. C., and Strong, J. C. 1992. Inspiratory deposition of ultrafine particles in human nasal replicate cast. *J. Aerosol Sci*. 23:65–72.

Tjälve, H., and Henriksson, J. 1999. Uptake of metals in the brain via olfactory pathways. *NeuroToxicity* 20(2–3):181–196.

Ueno, M., Akiguchi, I., Hosokawa, M., Kotani, H., Kanenishi, K., and Sakamoto, H. 2000. Blood–brain barrier permeability in the periventricular areas of the normal mouse brain. *Acta Neuropathol*. 99:385–392.

U.S. Environmental Protection Agency. 1996. *Air quality criteria for particulate matter*. Research Triangle Park, NC: National Center for Environmental Assessment–RTP Office. Report EPA/600/P95/001aF-cF.3v.

Vale, R. D., Reese, T. S., and Sheetz, M. P. 1985. Identification of a novel force-generating protein, kinesin, involved in microtubule-based motility. *Cell* 42:39–50.

von Klot, S., Wölke, G., Tuch, T., Heinrich, J., Dockery, D. W., Schwartz, J., Kreyling, W. G., Wichmann, H. E., and Peters, A. 2002. Increased asthma medication use in association with ambient fine and ultrafine particles. *Eur. Respir. J*. 20:691–702.

Wichmann, H.-E., Spix, C., Tuch, T., Wölke, G., Peters, A., Heinrich, H., Kregling, W. G., and Heyder, J. 2000. *Daily mortality and fine and ultrafine particles in Erfurt, Germany. Part I: Role of particle number and particle mass.* Health Effects Institute Research Report No. 98, November.

Woo, K.-S., Chen, D.-R., Pui, D. Y. H., and McMurry, P. H. 2001. Measurement of Atlanta aerosol size distributions: Observations of ultrafine particle events. *Aerosol Sci. Technol*. 34:75–87.